



Lasers in Manufacturing Conference 2015

## Laser micro structuring using adaptive mirror for extra-cavity beam shaping of high-power ultra-short laser pulses

Marco Smarra<sup>a\*</sup>, Johannes Neyer<sup>a</sup>, Klaus Dickmann<sup>a</sup>, Jean Pierre Bergmann<sup>b</sup>

<sup>a</sup>Laser Center Muenster University of Applied Sciences, Stegerwaldstraße 39, 48565 Steinfurt, Germany

<sup>b</sup>Technische Universität Ilmenau, Department of Production Technology, Neuhaus 1, 98684 Ilmenau, Germany

---

### Abstract

In laser micro processing there is a demand of shaped beams to improve the ablation results. Beam shaping is used e.g. for generating isolation grooves in solar cells. In addition the variation of the beam profile allows modifications of the surface properties of the processed material. These modifications can result in surface functionalization e.g. hydrophobic behavior. Phase changing optical elements are used to influence the wave-front and vary the beam shape. For high-power laser applications these elements have to be compliant with large pulse energies or high average power. A deformable mirror is one of the most suitable tools for the application with high power lasers, because of the absence of intensity losses due to diffraction. In this study a unimorph deformable mirror was used for beam-shaping during a picosecond laser ablation on metals and dielectrics. A piezoelectric disc behind the deformable mirror is separated into 35 segments, which can be individually driven by a voltage from -100 V up to 250 V. This feature allows complex deformation of this mirror which results in an individual variation of the spot geometry. The generation of different focus geometries, e.g. elliptical or line geometries, were analyzed. For this purpose on one hand the intensity profile and the beam propagation and on the other hand the influence to the surface modifications were studied. Another field of application for deformable mirrors is the variation of the focus position. By using additional optical components a controllable focus shift of 5 mm with a step size down to 25  $\mu\text{m}$  was realized. This feature was required to keep a continuous spot size on the ablation surface. The influence of this defined defocusing during the ablation process was analyzed and compared to a focus shift realized by a motorized translation axis. It could be shown that beam-shaping based on a deformable mirror is a precise method for intensity variations of the laser spot and focus shifting without loss of intensity.

*Keywords:* micro processing; ablation; surface functionalization

---

\* Corresponding author. Tel.: +49 2551 962-324; fax: +49 2551 962-490.  
E-mail address: marco.smarra@fh-muenster.de

## 1. Introduction

Laser micro processing using high power ultra-short laser pulses is a rapidly growing technology field. Due to the short interaction time, it is suitable for material processing with low thermal influence. There is a wide range of applications, such as cutting, drilling and ablating material, Hendricks et al., 2015, Finger et al., 2014, Fadeeva et al., 2013. The most common beam shape is a Gaussian beam. Runge et al. reported in 2013, that for laserscribing in thin Indium tin oxide films (150  $\mu\text{m}$ ) the process speed can be enhanced by the factor of 9 with 'a comparable quality'. This was realized changing the beam profile from a Gaussian profile to a top-hat profile. The generation of a top-hat profile can be achieved by using a diffractive optical element. The transmission efficiency of a focused beam shaper was determined by Jäger, 2014, to be better than 95 %. Using shaped beams can also enhance the processing speed by parallel processing, Gillner 2013, Bauer 2013. Diffractive optical elements can be fixed for example a grating or variable like spatial light modulators (SLM). The reflectivity of commercial available modulators is about 60-80%. If working with transitive spatial light modulators the transmission efficiency may be even lower. To use the whole intensity of the beam, refractive elements offer a high potential. 2014 Dietlicher and Eberle reported about a deformable lens for focus variation. They used an adaptive lens which can be deformed by a liquid filled polymer membrane.

The combination of a high flexibility influence to the incident beam and a high transformation efficiency is demonstrated in this paper by using a deformable mirror. This mirror is more flexible than a static diffractive optical element and transforms > 99.9 % of the incident beam because of its uniform surface.

## 2. Experimental setup

### 2.1 Deformable mirror

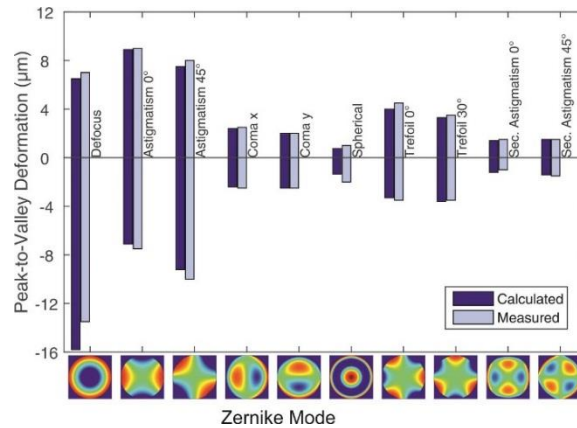


Fig. 1. Peak-to-Valley values for the Zernike Modes 3-12. The defocus deformation can be varied in the range of [-13  $\mu\text{m}$  to +7  $\mu\text{m}$ ].

For this study a bimorph deformable mirror was used. This type of mirror was produced by combining a piezoelectric ceramic with a mirror substrate. Piezoelectric materials deform themselves by a supply voltage. By separating the ceramic into individual addressable segments the deformation of the surface can be controlled precisely. The mirror used in this study is separated into 35 segments. Each segment can be controlled by a driven voltage between -100 V and +250 V. This voltage range is divided into 4000 steps. The deformation of the surface was determined by a phase-shift interferometer and described by a combination of Zernike

coefficients. These coefficients describe e.g. the tilt and defocus of the surface. Fig. 1 shows the peak-to-valley deformation for the Zernike coefficients 3 to 12 (from defocus to secondary astigmatism) that can be achieved.

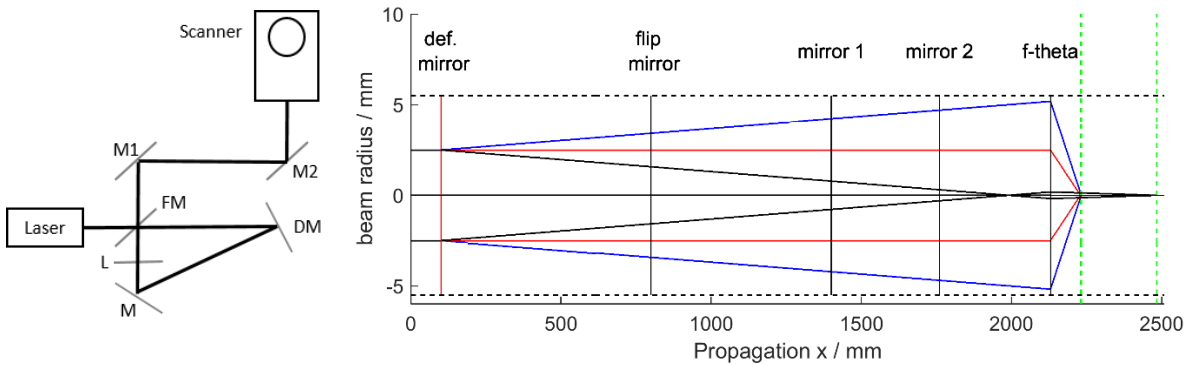
Using the Zernike coefficients to describe the deformation of the mirror surface is a common way to control the deformable mirror. The coefficient for defocus allows to set the radial deformation of the mirror. The surface equals a concave or convex mirror. The focal length ( $f$ ) depends on the deflection of the surface and can be calculated via equation (1) by the knowledge of the Zernike induced defocus deformation of the mirror ( $Z_{Def}$  in  $\mu\text{m}$ ) and the mirror diameter  $D$ :

$$f = \frac{D^2}{32 \cdot Z_{Def}} \quad (1)$$

The aperture of the mirror is 10 mm. These values result in focal length from minus infinity to -240 mm and from +450 mm to positive infinity – a deformation of 0  $\mu\text{m}$  results in a flat mirror surface with a focal length of infinity. A negative value for the defocus coefficient results in a convex lens behavior and a positive in a concave lens behavior.

## 2.2 Optical system design

The test system for this study included a picosecond-laser ( $\lambda = 1030 \text{ nm}$ ,  $\tau \approx 8 \text{ ps}$ ,  $P = 50 \text{ W}$ ,  $f = 800 \text{ kHz}$ ). The beam was positioned to the work piece by a scanning system (Hurryscan II) and was focused by an f-theta lens with a focal length of 100 mm. The beam path included a flip mirror (FM) to switch between the path using the original beam and the path using the deformable mirror (DM). For setup and study reasons the length of the beam path between laser exit and scanner entrance is about 2 meters, see Fig. 2, left. The setup also includes two mirrors (M1, M2) which are positioned in this 2 m long beam path. It is important that the beam is not focused onto these mirrors, because this may destroy them, although they are coated to reflect high intensity



beams.

Fig. 2. Left: Top view of the beam path: There are two possible ways of propagation – in order to switch between original beam profile and deformed profile there is a flip mirror (FM) after the exit of the laser. Right: Ray tracing analysis with deformable mirror and f-theta lens for Zernike coefficients defocus -2 (blue), 0 (red) and +2 (black). The distance between minimal and maximal focus position is about 254 mm with nonlinear steps.

An ABCD-matrix method was used to calculate the beam propagation. As equation (1) shows, the mirror can be replaced by a lens. A concave lens results in a focusing and a convex lens in a defocussing influence to the beam. Fig. 2 shows a ray tracing analysis of the beam propagation for Zernike defocus coefficients of -2, 0 and +2 (blue, red and black lines). The maximal beam radius is 5.5 mm due to the aperture of the scanner,

indicated by dashed lines. To avoid intensity losses at the scanner entrance the beam diameter was set to 5 mm before passing the deformable mirror. The beam diameter cannot be reduced furthermore because of the minimal size of active elements of the mirror. A defocus coefficient of 0 results in a flat mirror, without any influence to the beam and leads to a nominal focus length of 100 mm. If the mirror defocusses (values less than 0) the focus length growth slightly. For a defocus coefficient greater than 1.9 the beam is focused before passing the f-theta lens. This results in a distant focus position behind the f-theta lens. There is no linearity in this type of focus shifting.

An additional lens (A) reduce the focal range and the step size. The ray tracing result is shown in Fig. 3. The values for the Zernike coefficient are limited to  $[-2; 3]$  to avoid focused beams on the mirrors 1 or 2. The focal length of the system is determined to be 111 mm for a flat deformable mirror (Zernike value for defocus coefficient = 0).

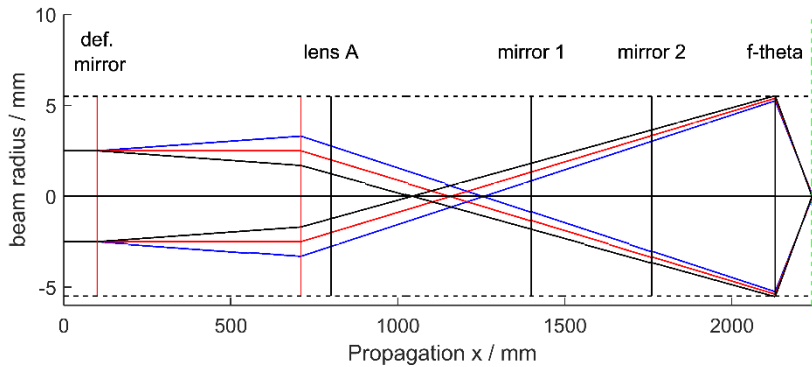


Fig. 3. Ray tracing analysis with deformable mirror and additional lens to transform the beam angle. This reduces the focal range and the step size of the focal shift. The distance of minimal and maximal focus position is about 3 mm with linear steps in between.

### 2.3 Beam analysis

Along the beam propagation the intensity profile was investigated with a combination of CCD-camera and a microscope objective. Therefore every 50  $\mu\text{m}$  a picture was taken and these pictures were analyzed by a beam analyzing software. The software calculates the minimal waist radius and the Rayleigh-length. This setup is also used to analyze different beam shapes.

### 2.4 Laser ablation

The defocussed laser beam was used to generate small cavities in steel. The variation of focus position relative to the surface of the probe may result in a higher ablation rate than in the focus position. This phenomena was used to compare the ablation results of a focus shift realized by a translation axis to a focus shift realized by the deformable mirror: At first the probe was positioned to different defocus positions by the translation axis while the mirror defocus coefficient was set to 0. The cavities were ablated and the depth of these cavities was measured. After that the probe was set to defocus position of 0 by the axis and the mirror defocus coefficient was set to different defocus positions. Again cavities were ablated and the depth was measured. The topography of the laser ablated surfaces were analyzed by a chromatic sensor. This sensor has a measurement range of 3 mm with an accuracy of 1  $\mu\text{m}$ . The surface was scanned by this sensor and the ablation depth was investigated.

### 3. Results

#### 3.1 Focus geometries

The generation of different focus geometries was analyzed. The original shape is shown in Fig. 4, left. Other shapes like lines (middle) or triangle (right) shapes can be realized by combining different Zernike coefficients. There is a loss of intensity due to diffraction when generating complex geometries, like a trefoil.

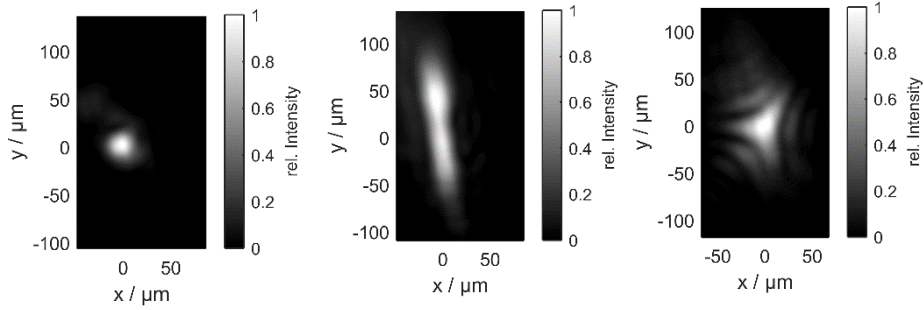


Fig. 4: Generation of different focus geometries: Left: Original Beam, Mid: Line, Right: Trefoil / Triangle.

#### 3.2 Focus shift

The focus shift realized by the deformable mirror was measured in a Zernike Defocus range of  $[-2; 3]$ . For each Zernike value the beam profile was analyzed and the waist position was determined, see Table 1. It shows the mirror deformation and the resulting focus variation. There is a strong linearity in the range of  $[-2; 2]$  but a deviation for Zernike values above 2. Nevertheless this table can be used as a look-up-table to vary the focus in a range of about 5 mm. The calculated step size for the focus variation is  $0.005 \mu\text{m}$ . Due to creep and hysteresis effects a statistic variation of  $25 \mu\text{m}$  was determined.

Table 1. Determined focus position when defocussing the beam using a deformable mirror and the transmitted power in relation to focus position 0.

Zernike Value Defokus	Focus Position (mm)	Focus Diameter ( $\mu\text{m}$ )
-2	-2.02	52
-1	-1.03	50
0	0.00	53
1	0.99	50
2	1.89	49
3	2.62	48

### 3.3 Ablation results

The ablation results of a defocus performed by the translation axis (red) and the deformable mirror (blue) were compared in Fig. 5. It is demonstrated, that for different defocus positions the ablation depth for axis and mirror are nearly the same.

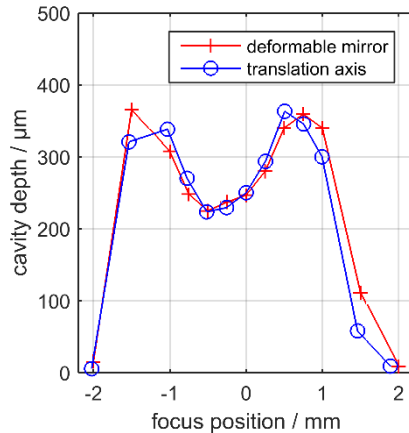


Fig. 5: Comparison of the ablation results with focus shift. Comparison of the realization by translation axis (circle) to those realized by a deformable mirror (cross). The maximal ablation can be realized by a defocus position of 0.75 mm or -1.25 mm.

## 4. Conclusion and Outlook

It was shown that a focus shift can be realized by a deformable mirror. An ABCD method was used to calculate an additional lens that transform the beam angle. This was necessary to realize a linear focus shift with a step size of about 25 μm and to reduce the range to about 5 mm. To avoid intensity losses at the scanner entrance the beam diameter was reduced to 5 mm. The spot diameter of the shifted beams is about 50 μm. The ablation results for the generation of different focus positions by the translation axis and the deformable mirror show comparable cavity depth.

Future work will need to enlarge the range and the linearity of the focus shift. In addition a long term study concerning the behavior of the mirror during laser processing will be the next investigations.

## References

- Hendricks, F., Patel, R. Matylitsky, V. V., "Micromachining of bio-absorbable stents with ultra-short pulse lasers" in Proc. SPIE 9355, Frontiers in Ultrafast Optics: Biomedical Scientific and Industrial Applications XV, 935502.
- Finger, J., Reininghaus, M., 2013, "Effects of pulse to pulse interactions on ultra-short laser drilling of steel with repetition rates up to 10 MHz" in Opt. Express 22, 18790-18799
- Fadeeva, E., Deiwick, A. Chichkov, B., Schlie-Wolter, S. 2014, „Impact of laser-structured biomaterial interfaces on guided cell response“ in "Interface Focus" 1 (4), 20130048
- Runge, S., Rexhepi, M., Bischoff, C., Hellman, R., 2013, "Laserscribing of Thin Films Using Top-Hat Laser Beam Profiles" in „Journal of Laser Micro/Nanoengineering“ Vol. 8, No. 3, p. 309.
- Jäger, E., Rädcl, U., Bischoff, C., Umhofer, U., Rung, S., Hellmann, R., 2014 "Laser micromachining – parallel processing with multiple top hat beams"
- Bauer, L., 2013, „Materialbearbeitung mit strahlgeformten Pikosekunden-Laserpulsen“, UKP Workshop Aachen
- Gillner, A., 2013, „UKP am Fraunhofer ILT - Laser, Prozesse und Systeme“, UKP Workshop Aachen
- Dietlich, M., Eberle, G., 2014, Laserfokussierung mit fokusvariabler Linse in „Laser“ Vol. 2, 2014, p. 26